Joint Beamforming and Resource Allocation for Integrated Satellite-Terrestrial Networks

Girim Kwon*, Wonjae Shin†, Andrea Conti‡, William C. Lindsey§, and Moe Z. Win*
*Wireless Information and Network Sciences Laboratory, Massachusetts Institute of Technology, Cambridge, MA 02139, USA
†Department of Electrical and Computer Engineering, Ajou University, Suwon-si, Gyeonggi-do, 16499, South Korea
‡Department of Engineering and CNIT, University of Ferrara, 44122 Ferrara, Italy
§Ming Hsieh Department of Electrical Engineering, University of Southern California, Los Angeles, CA 90089, USA
Email: girimk@mit.edu, wjshin@ajou.ac.kr, a.conti@ieee.org, wclindsey@gmail.com, moewin@mit.edu

***Abstract*—Integrated satellite-terrestrial networks (ISTNs) are essential for providing ubiquitous mobile ultra-broadband service in beyond 5G networks. The spectral efficiency and reliability of ISTN depend on the integrated architecture and its operational strategies including interference management and resource allocation. Our view is to integrate terrestrial access and satellite backhaul networks and to develop an optimization technique for their joint operation. This paper proposes an efficient integrated access and backhaul (IAB) architecture for satellite-terrestrial networks (STNs) based on reverse time division duplexing (TDD) considering both uplink (UL) and downlink (DL). In particular, in-band backhauling and gNodeB (gNB) cooperation are considered for high spectral efficiency and reliability. A framework for joint optimization of cooperative beamforming and resource allocation is developed to maximize the UL-DL rate region of the in-band IAB. The proposed scheme is verified using the 3rd Generation Partnership Project (3GPP) standard channel models. Results show that the proposed scheme significantly outperforms the conventional wireless backhauling, while approaching to an outer bound of the UL-DL rate region.**

***Index Terms*—Integrated satellite-terrestrial networks (ISTN), satellite backhaul, integrated access and backhaul (IAB), reverse time division duplexing (TDD).**

ICC 2023 - IEEE International Conference on Communications | 978-1-5386-7462-8/23/$31.00 ©2023 IEEE | DOI: 10.1109/ICC45041.2023.10278943

I. Introduction

Non-terrestrial networks are expected to play a key role in vertical domain expansion of beyond fifth generation (5G) mobile communications and have been under exploration in 3rd Generation Partnership Project (3GPP) [1]–[3]. Vertical domain expansion is crucial to support global broadband coverage for ubiquitous mobile ultra-broadband service, which is one of the potential service classes in beyond 5G communications. Enabling techniques for this service include the advanced backhaul connections using the millimeter wave (mmWave) band and the integrated satellite-terrestrial networks (ISTNs) [3], [4]. To establish the global broadband coverage, advanced geostationary orbit (GEO) satellite constellations (e.g., Viasat's *ViaSat-3* and Inmarsat's *Inmarsat-6*) are expected. Low earth orbit (LEO) satellite constellations (e.g., SpaceX, Amazon, OneWeb, Telesat, and Boeing) are also being formed in the industry.

As one of various ISTN implementations, integrated access and backhaul (IAB) architecture is a key for providing global broadband coverage by combining terrestrial access networks with satellite backhauls, particularly for urban hotspot, disaster area, and isolated rural areas [5], [6]. For example, satellite-terrestrial networks (STNs) with IAB can achieve a higher capacity than direct satellite access by exploiting high transmit power and beamforming (BF) gain of terrestrial gNodeBs (gNBs). The satellite backhaul also benefits from flexible and cost-effective network operation.

Wireless backhauling has received attention in the area of terrestrial networks due to easy installation and flexible operation, which has been standardized under the name of IAB in 3GPP [7]–[10]. Wireless backhaul systems can be deployed with either out-of-band backhauling or in-band backhauling. The works in [9], [10] have shown that in-band backhauling is more resource-efficient than out-of-band backhauling. These works have focused on downlink (DL) BF design assuming a base station-centric user association in the access networks. To enable the global broadband connectivity, a spectrally efficient BF scheme for STNs with in-band IAB is needed.

BF design for terrestrial-satellite networks has been largely studied in recent years [11]–[15]. The work in [11] designed a multi-user BF scheme for the satellite communication system without consideration of coexistence or integration with terrestrial networks. The works in [12]–[14] have considered coexistence of the satellite access network and terrestrial access network. They have considered the satellite as a separate base station serving users rather than as a wireless backhaul. The work in [15] designed a BF scheme for the in-band IAB in STNs with an earth station. However, it only considered the DL transmission with a single base station. For spectrally efficient in-band IAB, joint optimization of BF and resource allocation is needed in the STNs that accounts for both uplink (UL) and DL characteristics.

This paper proposes an in-band IAB architecture for STNs considering both UL and DL. We develop a framework for joint optimization of cooperative BF and resource allocation. We advocate the use of reverse time division duplexing (TDD)-based IAB, which enables spectrally-efficient STNs. The key contributions are as follows:

- we propose an IAB architecture for mmWave STNs based on reverse TDD and gNB cooperation, which enables a spectrally efficient in-band backhauling;
- we design an optimization algorithm that maximizes the weighted sum of UL and DL rates, which can enlarge the

UL-DL rate region of STNs; and
- we quantify the gain of the proposed in-band IAB scheme over the conventional orthogonal backhaul scheme using 3GPP channel models.

Notations: A random variable and its realization are denoted by x and x, respectively. A random vector and its realization are denoted by $\mathbf{x}$ and $\boldsymbol{x}$, respectively. The m-by-m identity matrix is denoted by $\boldsymbol{I}_m$. The transpose and conjugate transpose are denoted by $(\cdot)^{\mathrm{T}}$ and $(\cdot)^{\dagger}$, respectively.

II. System Model

A. In-band IAB for STNs

Consider an STN with a single GEO satellite providing wireless backhaul links to a terrestrial network within the area of a single satellite beam. The terrestrial network consists of B gNBs and U user equipments (UEs). The gNBs are equipped with an antenna array of M elements, while the UEs have a single antenna. The gNBs cooperatively transmit/receive the signals to/from the satellite and UEs by exploiting the multi-node diversity and BF gain. The STN is assumed to operate in mmWave band, e.g., *Ka*-band, which is suitable for providing potential broadband services. In the mmWave STN, we assume that direct links between the satellite and UEs are not considered due to limited link budget.

We adopt the in-band operation between the backhaul and access links with interference management. Resource allocation and BF are optimized considering both the UL and DL.

B. Reverse TDD for STNs with IAB

For efficient channel usage, resource allocation is necessary according to UL and DL traffic demands. In this regard, 5G New Radio (NR) uses various UL-DL configurations for TDD. Particularly for the in-band IAB, we adopt the reverse TDD as in Fig. 1, which is useful for interference management between the backhaul and access links [16]. At time slot 1, the backhaul DL and access UL signals are transmitted from the satellite and the UEs to the gNBs. At time slot 2, the backhaul UL and access DL signals are transmitted from the gNBs to the satellite and the UEs. In this way, self interference is avoided using half duplex gNBs, and interference between backhaul and access is mitigated by gNB BF. The time fractions τ and $1-\tau$ are allocated to the time slots 1 and 2.

The reverse TDD is useful in STNs to take into account a long propagation delay in the non-terrestrial channel. The conventional TDD system requires a guard period between DL and UL that equals to the maximum round trip propagation delay. This is not applicable to the network with a GEO satellite because of a long propagation delay, e.g., 119.29 ms for a one-way at the elevation angle of 90°. Instead, in the reverse TDD-based IAB system, a TDD frame length can be chosen to be a fraction of the long propagation delay so that the UL and DL signals can be transmitted consecutively in separated time slots [17].

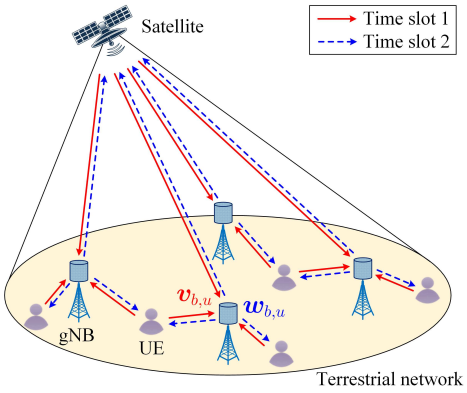

Fig. 1. The proposed STN with in-band IAB based on the reverse TDD and gNB cooperation.

C. Non-Terrestrial and Terrestrial Channel Models

The backhaul DL channel from the satellite to the bth gNB and the access UL channel from the uth UE to the bth gNB are commonly expressed by an $M \times 1$ vector as

$$\mathbf{h}_{b,u} = \xi_{b,u}\boldsymbol{\omega}_{b,u} \tag{1}$$

for $b = 1, 2, \ldots, B$ and $u = 0, 1, \ldots, U$, where $u = 0$ indicates the satellite, while $u \geqslant 1$ indicates the UEs. $\xi_{b,u}$ and $\boldsymbol{\omega}_{b,u}$ denote the large- and small-scale channels, respectively. Based on TDD reciprocity, the backhaul UL and access DL channels are denoted by $\mathbf{h}_{b,u}^{\dagger}$. We adopt the 3GPP models in [18], [19] for both the non-terrestrial and terrestrial links.

Both $\xi_{b,u}$ and $\boldsymbol{\omega}_{b,u}$ in (1) depend on the existence of the line-of-sight (LOS) path, which is modeled as the Bernoulli random variable $\chi_{b,u} \in \{0, 1\}$ with respect to the LOS probability. The LOS probability is a function of the elevation angle α_b between the satellite and the bth gNB [18] or the distance $d_{b,u}$ between the bth gNB and the uth UE [19].

The large-scale channel in (1) is given by $\xi_{b,u} = \sqrt{G_{b,u}^{\mathrm{TX}} G_{b,u}^{\mathrm{RX}} / \mathsf{L}_{b,u}}$ with $\mathsf{L}_{b,0} = A_{b,0}^{\mathrm{FS}}\, \mathsf{A}_{b,0}^{\mathrm{SF}}\, \mathsf{A}_{b,0}^{\mathrm{CL}}\, A_{b,0}^{\mathrm{G}}\, A_{b,0}^{\mathrm{S}}$ for $u = 0$ and $\mathsf{L}_{b,u} = A_{b,u}^{\mathrm{FS}}\, \mathsf{A}_{b,u}^{\mathrm{SF}}$ for $u \geqslant 1$. $G_{b,u}^{\mathrm{TX}}$ and $G_{b,u}^{\mathrm{RX}}$ denote the transmit and receive antenna gains, respectively. Those for the satellite are determined by the beam pattern as a function of α_b. The attenuation terms in $\mathsf{L}_{b,u}$ depend on $\chi_{b,u}$, α_b, $d_{b,u}$, and the frequency f_{c}. Specifically, $A_{b,u}^{\mathrm{FS}}$ is the free space path loss, $\mathsf{A}_{b,u}^{\mathrm{SF}}$ is the shadow fading loss, $\mathsf{A}_{b,0}^{\mathrm{CL}}$ is the clutter loss, $A_{b,0}^{\mathrm{G}}$ is the atmospheric loss, and $A_{b,0}^{\mathrm{S}}$ is the scintillation loss.

The small-scale channel in (1) is given by $\boldsymbol{\omega}_{b,u} = \boldsymbol{\omega}_{b,u}^{(\mathrm{L})}$ if $\chi_{b,u} = 1$ and $\boldsymbol{\omega}_{b,u} = \boldsymbol{\omega}_{b,u}^{(\mathrm{N})}$ if $\chi_{b,u} = 0$ where $\boldsymbol{\omega}_{b,u}^{(\mathrm{L})} \triangleq \sqrt{\kappa_{b,u}/(\kappa_{b,u}+1)}\boldsymbol{a}\big(\phi_{b,u}, \theta_{b,u}\big) + \sqrt{1/(\kappa_{b,u}+1)} \sum_{k=1}^{K_{b,u}} \sum_{n=1}^{N_{b,u}} \sqrt{\varrho_{b,u}^{(k)}/N_{b,u}}\, \beta_{b,u}^{(k,n)}\, \boldsymbol{a}\big(\varphi_{b,u}^{(k,n)}, \theta_{b,u}^{(k,n)}\big)$ and $\boldsymbol{\omega}_{b,u}^{(\mathrm{N})} \triangleq \sum_{k=1}^{K_{b,u}} \sum_{n=1}^{N_{b,u}} \sqrt{\varrho_{b,u}^{(k)}/N_{b,u}}\, \beta_{b,u}^{(k,n)}\, \boldsymbol{a}\big(\varphi_{b,u}^{(k,n)}, \theta_{b,u}^{(k,n)}\big)$. $\boldsymbol{\omega}_{b,u}^{(\mathrm{L})}$ includes a LOS path and clustered non-line-of-sight (NLOS) paths, while $\boldsymbol{\omega}_{b,u}^{(\mathrm{N})}$ includes only NLOS paths. The Rician K factor is denoted by $\kappa_{b,u}$. For given $\chi_{b,u}$, the NLOS paths form $K_{b,u}$ clusters each with $N_{b,u}$ rays and the normalized power $\varrho_{b,u}^{(k)}$ such that $\sum_k \varrho_{b,u}^{(k)} = 1$ [19]. The complex path gain is denoted by $\beta_{b,u}^{(k,n)}$. The array response

vector of the gNB is denoted by $\boldsymbol{a}(\cdot)$. The azimuth and zenith angles are denoted by $\phi_{b,u}$ and $\theta_{b,u}$ for the LOS path; by $\varphi_{b,u}^{(n,m)}$ and $\theta_{b,u}^{(n,m)}$ for the random NLOS paths, respectively.

D. Signal-to-Interference-plus-Noise Ratio (SINR)

The gNBs are assumed to obtain the channel state information using pilot signals transmitted from the satellite and UEs. These information are shared among the gNBs and used for cooperative BF in both time slots 1 and 2 based on the channel reciprocity. Since the relative positions of the GEO satellite and gNBs are fixed, the channel coherence time of the satellite backhaul link is assumed to be larger than the round-trip propagation time.

At time slot 1, the received signals at the gNBs are jointly combined with the BF vectors $\boldsymbol{v}_{b,u}, \forall b$ for each $u \in \{0,1,\ldots,U\}$. The SINRs for the backhaul DL and access UL are expressed by

$$\gamma_u' = \frac{\left|\sum_{b=1}^{B}\sqrt{P_u'}\boldsymbol{v}_{b,u}^{\dagger}\boldsymbol{h}_{b,u}\right|^2}{\sum_{\substack{j=0,\\ j\neq u}}^{U}\left|\sum_{b=1}^{B}\sqrt{P_j'}\boldsymbol{v}_{b,u}^{\dagger}\boldsymbol{h}_{b,j}\right|^2+(\sigma')^2\sum_{b=1}^{B}\|\boldsymbol{v}_{b,u}\|^2} \quad (2)$$

where $u=0$ indicates the backhaul DL, and $u \geqslant 1$ indicates the access UL. P_u' is the transmit power of the satellite and the uth UE. $(\sigma')^2$ is the noise power at the gNB.

At time slot 2, the SINRs for the backhaul UL at the satellite and the access DL at the uth UE are expressed by

$$\gamma_u = \frac{\left|\sum_{b=1}^{B}\sqrt{P_{b,u}}\boldsymbol{h}_{b,u}^{\dagger}\boldsymbol{w}_{b,u}\right|^2}{\sum_{j=0,j\neq u}^{U}\left|\sum_{b=1}^{B}\sqrt{P_{b,j}}\boldsymbol{h}_{b,u}^{\dagger}\boldsymbol{w}_{b,j}\right|^2+\sigma_u^2} \quad (3)$$

where $u=0$ indicates the backhaul UL, and $u \geqslant 1$ indicates the access DL. The transmit power and BF vector at the bth gNB for the satellite and the uth UE are denoted by $P_{b,u}$ and $\boldsymbol{w}_{b,u}$, respectively. The total transmit power at each gNB is limited by $\sum_{u=0}^{U}\|\boldsymbol{w}_{b,u}\|^2 P_{b,u} \leqslant P^{\star}$. σ_u^2 is the noise power.

E. Optimal Receive BF at gNBs

Considering fixed transmit powers of the satellite and UEs, the receive BF $\boldsymbol{v}_{b,u}, \forall b,u$ is optimized as follows. First, define two concatenated vectors as $\boldsymbol{h}_u \triangleq [\boldsymbol{h}_{1,u}^{\mathrm{T}}, \boldsymbol{h}_{2,u}^{\mathrm{T}}, \ldots, \boldsymbol{h}_{B,u}^{\mathrm{T}}]^{\mathrm{T}}$ and $\boldsymbol{v}_u \triangleq [\boldsymbol{v}_{1,u}^{\mathrm{T}}, \boldsymbol{v}_{2,u}^{\mathrm{T}}, \ldots, \boldsymbol{v}_{B,u}^{\mathrm{T}}]^{\mathrm{T}}$. From (2), the optimal receive BF at time slot 1 can be found for given $P_u', \forall u$ as

$$\boldsymbol{v}_u^{*} = \underset{\boldsymbol{v}_u}{\operatorname{argmax}} \frac{P_u'\boldsymbol{v}_u^{\dagger}\big(\boldsymbol{h}_u\boldsymbol{h}_u^{\dagger}\big)\boldsymbol{v}_u}{\boldsymbol{v}_u^{\dagger}\big(\sum_{j=0,j\neq u}^{U}P_j'\boldsymbol{h}_j\boldsymbol{h}_j^{\dagger}+(\sigma')^2\boldsymbol{I}_{MB}\big)\boldsymbol{v}_u} \quad (4)$$

which is the generalized Rayleigh quotient problem. The solution to (4) can be found by the dominant generalized eigenvector of the matrices $P_u'\boldsymbol{h}_u\boldsymbol{h}_u^{\dagger}$ and $\sum_{j=0,j\neq u}^{U}P_j'\boldsymbol{h}_j\boldsymbol{h}_j^{\dagger}+(\sigma')^2\boldsymbol{I}_{MB}$.

Using $\boldsymbol{v}_u^{*}, \forall u$ in (4), the achievable rates per unit bandwidth of the access UL and backhaul DL are given by $\tilde{R}^{\mathrm{UL}} \triangleq \sum_{u=1}^{U}\log_2\big(1+\gamma_u'(\boldsymbol{v}_u^{*})\big)$ and $\tilde{R}^{\mathrm{DL}} \triangleq \log_2\big(1+\gamma_0'(\boldsymbol{v}_0^{*})\big)$, respectively. Then the end-to-end achievable sum rates for the UL and DL of the network are determined by the minimum of the backhaul and access links, which can be expressed as

$$R^{\mathrm{UL}} = \min\big\{\tau\tilde{R}^{\mathrm{UL}},\,(1-\tau)\log_2\big(1+\gamma_0\big)\big\} \quad (5a)$$

$$R^{\mathrm{DL}} = \min\big\{\tau\tilde{R}^{\mathrm{DL}},\,(1-\tau)\textstyle\sum_{u=1}^{U}\log_2\big(1+\gamma_u\big)\big\}. \quad (5b)$$

where τ is the time fraction between the time slots 1 and 2.

III. Optimization Framework

A. Joint Optimization Problem

To maximize the UL-DL rate region of the STN with IAB, the transmit BF and power allocation at the gNBs should be jointly optimized with time allocation for every channel coherence time. First, the set of the BF vectors and power allocation and their power constraint are defined by

$$\mathcal{S} \triangleq \big\{\boldsymbol{w}_{b,u}, P_{b,u} : b=1,2,\ldots,B, u=0,1,\ldots,U\big\} \quad (6)$$

$$\check{\mathcal{S}}_0 \triangleq \big\{\mathcal{S} : \textstyle\sum_{u=0}^{U}\|\boldsymbol{w}_{b,u}\|^2 P_{b,u} \leqslant P^{\star}, \text{ and } P_{b,u} \geqslant 0, \forall b\big\}. \quad (7)$$

Using (6), the SINRs in (3) can be expressed as a function of $\mathcal{S}$, i.e., $\gamma_u(\mathcal{S})$. Then we aim to maximize the weighted sum of R^{UL} and R^{DL} using (5), which is defined as

$$f(\mathcal{S},\tau) \triangleq \zeta\min\big\{\tau\tilde{R}^{\mathrm{UL}},(1-\tau)\log_2\big(1+\gamma_0(\mathcal{S})\big)\big\} + (1-\zeta)\min\big\{\tau\tilde{R}^{\mathrm{DL}},(1-\tau)\textstyle\sum_{u=1}^{U}\log_2\big(1+\gamma_u(\mathcal{S})\big)\big\} \quad (8)$$

where ζ is a known weight for controlling the trade-off between the UL and DL rates. From (6), (7), and (8), the optimization problem is formulated as

$$\mathscr{P}_0: \underset{\mathcal{S}\subseteq\check{\mathcal{S}}_0, 0<\tau<1}{\text{maximize}} \quad f(\mathcal{S},\tau).$$

Solving $\mathscr{P}_0$ for different ζ will give an UL-DL rate region.

B. Optimization Strategy

To solve $\mathscr{P}_0$, a sequential maximization approach is used based on the fact that $\max_{\mathcal{S}\subseteq\check{\mathcal{S}}_0,0<\tau<1} f(\mathcal{S},\tau) = \max_{0<\tau<1}\max_{\mathcal{S}\subseteq\check{\mathcal{S}}_0} f(\mathcal{S},\tau)$. Then a two-step optimization is performed along with each variables, i.e., $\mathcal{S}$ and τ.

First, introduce the common power level p_u, which is commonly used at all the gNBs. Then the feasible constraint set $\check{\mathcal{S}}_0$ can be equivalently expressed by $\check{\mathcal{S}}_1 \triangleq \big\{\mathcal{S} : \|\boldsymbol{w}_u\|^2 = 1, \forall u, \sum_{u=0}^{U}\|\boldsymbol{w}_{b,u}\|^2 p_u \leqslant P^{\star}, \text{ and } P_{b,u}=p_u \geqslant 0, \forall b\big\}$ where $\boldsymbol{w}_u \triangleq [\boldsymbol{w}_{1,u}^{\mathrm{T}}, \boldsymbol{w}_{2,u}^{\mathrm{T}}, \ldots, \boldsymbol{w}_{B,u}^{\mathrm{T}}]^{\mathrm{T}}$ [20]. Using $\check{\mathcal{S}}_1$, the inner problem for optimizing $\mathcal{S}$ is expressed for given τ as

$$\mathscr{P}_1: \underset{\mathcal{S}\subseteq\check{\mathcal{S}}_1}{\text{maximize}} \quad f(\mathcal{S},\tau).$$

Since the end-to-end UL and DL rates in the first and second terms of (8) may be limited by $\tau\tilde{R}^{\mathrm{UL}}$ and $\tau\tilde{R}^{\mathrm{DL}}$, respectively, $\mathcal{S}$ should be designed such that the transmit power is not excessively allocated to one of the backhaul UL or the access DL. In other words, the power usage of the gNBs needs to be balanced between the backhaul UL and the access DL to maximize the objective value.

Our strategy is to firstly obtain an initial solution assuming no bottleneck in end-to-end links, i.e., $\tilde{R}^{\mathrm{UL}} = \infty$ and $\tilde{R}^{\mathrm{DL}} = \infty$ in $\mathscr{P}_1$. Then further optimization process will be conducted considering the bottleneck. The initial problem can be seen as the conventional weighted sum rate maximization problem, $\mathring{\mathscr{P}}_1 : \max_{\mathcal{S}\subseteq\check{\mathcal{S}}_1} \mathring{f}(\mathcal{S})$ where $\mathring{f}(\mathcal{S}) = \zeta\log_2(1+\gamma_0(\mathcal{S}))+(1-\zeta)\sum_{u=1}^{U}\log_2(1+\gamma_u(\mathcal{S}))$, which can be solved by using the existing algorithm in [20]. Once the initial solution is obtained as $\mathring{\mathcal{S}}$ from $\mathring{\mathscr{P}}_1$, the problem $\mathscr{P}_1$ can be modified to

a constrained maximization problem depending on the values of $\mathring{\mathcal{S}}$ and τ. Specifically, substituting $\mathring{\mathcal{S}}$ into $f(\mathcal{S},\tau)$ can give four different cases of formulating a constrained problem, namely, Case A, Case B, Case C, and Case D, according to the behaviors of the two minimum functions.

- Case A represents a condition in which $\tau \in \mathcal{T}_{\mathrm{A}}(\mathring{\mathcal{S}})$ is satisfied where $\mathcal{T}_{\mathrm{A}}(\mathring{\mathcal{S}}) \triangleq \{\tau : (1-\tau)\log_2\big(1+\gamma_0\big(\mathring{\mathcal{S}}\big)\big) \geqslant \tau\tilde{R}^{\mathrm{UL}}$ and $(1-\tau)\sum_{u=1}^{U}\log_2\big(1+\gamma_u\big(\mathring{\mathcal{S}}\big)\big) < \tau\tilde{R}^{\mathrm{DL}}\}$. In this case, the access DL can be improved from the initial optimization result while keeping the same rate of the backhaul UL by solving the constrained problem,

$$\mathscr{P}_{1,\mathrm{A}}: \underset{\mathcal{S}\subseteq\check{\mathcal{S}}_1}{\text{maximize}} \quad \sum_{u=1}^{U}\log_2\big(1+\gamma_u(\mathcal{S})\big) \quad \text{subject to} \quad \log_2\big(1+\gamma_0(\mathcal{S})\big) \geqslant \tfrac{\tau}{1-\tau}\tilde{R}^{\mathrm{UL}}.$$

- Case B represents a condition in which $\tau \in \mathcal{T}_{\mathrm{B}}(\mathring{\mathcal{S}})$ is satisfied $\mathcal{T}_{\mathrm{B}}(\mathring{\mathcal{S}}) \triangleq \{\tau : (1-\tau)\log_2\big(1+\gamma_0\big(\mathring{\mathcal{S}}\big)\big) < \tau\tilde{R}^{\mathrm{UL}}$ and $(1-\tau)\sum_{u=1}^{U}\log_2\big(1+\gamma_u\big(\mathring{\mathcal{S}}\big)\big) \geqslant \tau\tilde{R}^{\mathrm{DL}}\}$. In this case, the backhaul UL can be improved while keeping the same rate of the access DL by solving

$$\mathscr{P}_{1,\mathrm{B}}: \underset{\mathcal{S}\subseteq\check{\mathcal{S}}_1}{\text{maximize}} \quad \log_2\big(1+\gamma_0(\mathcal{S})\big) \quad \text{subject to} \quad \sum_{u=1}^{U}\log_2\big(1+\gamma_u(\mathcal{S})\big) \geqslant \tfrac{\tau}{1-\tau}\tilde{R}^{\mathrm{DL}}.$$

- The other two cases, i.e., Case C and Case D, do not need further optimization processes because $\mathring{\mathcal{S}}$ is already optimal for the following reasons. For Case C, i.e., $(1-\tau)\log_2\big(1+\gamma_0\big(\mathring{\mathcal{S}}\big)\big) \geqslant \tau\tilde{R}^{\mathrm{UL}}$ and $(1-\tau)\sum_{u=1}^{U}\log_2\big(1+\gamma_u\big(\mathring{\mathcal{S}}\big)\big) \geqslant \tau\tilde{R}^{\mathrm{DL}}$, the objective value of $\mathscr{P}_1$ using $\mathring{\mathcal{S}}$ is determined as $\zeta\tau\tilde{R}^{\mathrm{UL}} + (1-\zeta)\tau\tilde{R}^{\mathrm{DL}}$, which cannot be improved anymore. For Case D, i.e., $(1-\tau)\log_2\big(1+\gamma_0\big(\mathring{\mathcal{S}}\big)\big) < \tau\tilde{R}^{\mathrm{UL}}$ and $(1-\tau)\sum_{u=1}^{U}\log_2\big(1+\gamma_u\big(\mathring{\mathcal{S}}\big)\big) < \tau\tilde{R}^{\mathrm{DL}}$, it can be seen that $\mathscr{P}_1$ becomes equivalent to $\mathring{\mathscr{P}}_1$.

In summary, the algorithm for the problem $\mathscr{P}_1$ can be designed by using $\mathring{\mathscr{P}}_1$, $\mathscr{P}_{1,\mathrm{A}}$, and $\mathscr{P}_{1,\mathrm{B}}$.

IV. Algorithm Design

A. Overall Algorithm for the problem $\mathscr{P}_0$

The problem $\mathscr{P}_0$ can be solved by finding an optimal τ while solving $\mathscr{P}_1$. First, the initial set $\mathring{\mathcal{S}}$ is determined by solving $\mathring{\mathscr{P}}_1$ regardless of τ. For a given τ of the main loop, the inner problem, i.e., $\mathscr{P}_1$, is solved according to the strategy explained in Sec. III-B. Since the objective function of $\mathscr{P}_0$ has a non-monotonic behavior with respect to τ, we use the ternary search algorithm to find a local extremum. In Sec. IV-B, the algorithms for $\mathscr{P}_{1,\mathrm{A}}$ are presented while those for $\mathscr{P}_{1,\mathrm{B}}$ are omitted due to the similarity and page limit.

B. Algorithms for the problem $\mathscr{P}_{1,\mathrm{A}}$

The problem $\mathscr{P}_{1,\mathrm{A}}$ is decomposed into two subproblems along with the two different design variables. First, the BF vectors, $\boldsymbol{w}_u, \forall u$, are optimized for fixed common power levels. Then the common power levels $p_u, \forall u$ are optimized for fixed BF vectors. The two subproblems, namely, $\mathscr{P}_{1,\mathrm{A}}^{\mathrm{BF}}$ and $\mathscr{P}_{1,\mathrm{A}}^{\mathrm{PL}}$, are alternately updated in an iterative manner.

Algorithm 1 BF optimization for the problem $\mathscr{P}_{1,\mathrm{A}}^{\mathrm{BF}}$

Require: $\tilde{R}^{\mathrm{UL}}, \boldsymbol{h}_{b,u}, p_u, \sigma_u^2, \forall b,u$
Set $\breve{\mu}$ to be a positive number
$\boldsymbol{w}_u \leftarrow \tilde{\boldsymbol{h}}_{u,u}/\|\tilde{\boldsymbol{h}}_{u,u}\|, \forall u$
while $\boldsymbol{w}_u, \forall u$ does not converge within max iteration **do**
  Update $\{\tilde{\boldsymbol{H}}_{j,u}, \rho_j, \gamma_j, \forall j,u\}$
  $(\breve{\mu}, \hat{\mu}) \leftarrow (0, \breve{\mu})$
  while μ does not converge **do**
    $\mu \leftarrow (\breve{\mu}+\hat{\mu})/2$
    Update $\boldsymbol{S}_u$ and $\boldsymbol{T}_u, \forall u$ using (14) and (15)
    $\boldsymbol{w}_u \leftarrow$ the dominant eigenvector of $\boldsymbol{S}_u - \boldsymbol{T}_u, \forall u$
    if $\log_2\Big(1+\frac{|\tilde{\boldsymbol{h}}_{0,0}^{\dagger}\boldsymbol{w}_0|^2}{\sum_{j=1}^{U}|\tilde{\boldsymbol{h}}_{0,j}^{\dagger}\boldsymbol{w}_j|^2+\sigma_0^2}\Big) > \frac{\tau}{1-\tau}\tilde{R}^{\mathrm{UL}}$ **then**
      $\hat{\mu} \leftarrow \mu$
    else
      $\breve{\mu} \leftarrow \mu$
    end if
  end while
end while
Return: $\boldsymbol{w}_u, \forall u$

1) BF optimization: For notational convenience, the effective channel from the gNBs to the uth UE (or satellite) with respect to p_j is defined as $\tilde{\boldsymbol{h}}_{u,j} \triangleq \big[\sqrt{p_j}\boldsymbol{h}_{1,u}^{\mathrm{T}}, \sqrt{p_j}\boldsymbol{h}_{2,u}^{\mathrm{T}}, \ldots, \sqrt{p_j}\boldsymbol{h}_{B,u}^{\mathrm{T}}\big]^{\mathrm{T}}$ for $u,j = 0,1,\ldots,U$. Then γ_u is expressed by a function of $\{\boldsymbol{w}_i\}_{i=0}^{U}$ in $\mathscr{P}_{1,\mathrm{A}}^{\mathrm{BF}}$. In addition, the constraint $\mathcal{S} \subseteq \check{\mathcal{S}}_1$ of $\mathscr{P}_{1,\mathrm{A}}$ is reduced to $\|\boldsymbol{w}_u\|^2 = 1, \forall u$ in $\mathscr{P}_{1,\mathrm{A}}^{\mathrm{BF}}$. A local optimal BF solution to the non-convex subproblem $\mathscr{P}_{1,\mathrm{A}}^{\mathrm{BF}}$ is found by using the Karush-Kuhn-Tucker (KKT) conditions. Omitting the detailed derivation, the following relation is obtained,

$$(\boldsymbol{S}_u - \boldsymbol{T}_u)\,\boldsymbol{w}_u = \lambda_u \boldsymbol{w}_u \tag{13}$$

for $u = 0,1,\ldots,U$, where matrices $\boldsymbol{S}_u$ and $\boldsymbol{T}_u$ are defined as

$$\boldsymbol{S}_u \triangleq \begin{cases} \mu\tilde{\boldsymbol{H}}_{0,0} & \text{for } u=0 \\ \tilde{\boldsymbol{H}}_{u,u} & \text{for } u \geqslant 1 \end{cases} \tag{14}$$

$$\boldsymbol{T}_u \triangleq \begin{cases} \sum_{j=1}^{U}\gamma_j\tilde{\boldsymbol{H}}_{j,0} & \text{for } u=0 \\ \sum_{j=1,j\neq u}^{U}\gamma_j\tilde{\boldsymbol{H}}_{j,u} + \mu\gamma_0\tilde{\boldsymbol{H}}_{0,u} & \text{for } u \geqslant 1 \end{cases} \tag{15}$$

with $\tilde{\boldsymbol{H}}_{j,u} \triangleq \tilde{\boldsymbol{h}}_{j,u}\tilde{\boldsymbol{h}}_{j,u}^{\dagger}/(\rho_j \ln 2)$, $\rho_j \triangleq \sum_{i=0}^{U}|\tilde{\boldsymbol{h}}_{j,i}^{\dagger}\boldsymbol{w}_i|^2 + \sigma_j^2$, and $\gamma_j \triangleq |\tilde{\boldsymbol{h}}_{j,j}^{\dagger}\boldsymbol{w}_j|^2/(\sum_{i=0,i\neq j}^{U}|\tilde{\boldsymbol{h}}_{j,i}^{\dagger}\boldsymbol{w}_i|^2 + \sigma_j^2)$. μ and λ_u are the KKT multipliers for the two constraints, respectively. It is worth noting that $\boldsymbol{S}_u$ in (14) corresponds to the desired channel component, while $\boldsymbol{T}_u$ in (15) can be seen as the weighted sum of leakage components from the uth UE or satellite to the other nodes. From (13) and the primal feasibility, $\|\boldsymbol{w}_u\|^2 = 1$, we have $\boldsymbol{w}_u^{\dagger}(\boldsymbol{S}_u - \boldsymbol{T}_u)\boldsymbol{w}_u = \lambda_u$. Hence, for each iteration of the algorithm, $\boldsymbol{w}_u$ can be updated by the dominant eigenvector of the matrix $\boldsymbol{S}_u - \boldsymbol{T}_u$ given by using $\rho_u, \forall u$ of the previous iteration. Using this update rule, an optimal μ can be found by the bisection method to meet the equality of the rate constraint in $\mathscr{P}_{1,\mathrm{A}}$. The algorithm to solve the BF subproblem is summarized in Algorithm 1.

2) Power level optimization: Define the effective channel gain for given BF vectors as $g_{u,j} \triangleq |\sum_{b=1}^{B}\boldsymbol{h}_{b,u}^{\dagger}\boldsymbol{w}_{b,j}|^2 = |\boldsymbol{h}_u^{\dagger}\boldsymbol{w}_j|^2$ for $u,j = 0,1,\ldots,U$. In addition, the constraint

Algorithm 2 Power level optimization for the problem $\mathscr{P}_{1,\mathrm{A}}^{\mathrm{PL}}$

Require: $\tilde{R}^{\mathrm{UL}}, P^{\star}, \boldsymbol{w}_{b,u}, \boldsymbol{h}_{b,u}, \sigma_u^2, \forall b, u$
Set $\check{\eta}$ and $\check{\nu}$ to be positive numbers
Initialize $p_u, \forall u$ with equal power allocation
Initialize $\nu_b, \forall b$ with $\check{\nu}$
while $p_u, \forall u$ does not converge within max iteration **do**
  Update $\{q_u, t_u, s_u, \forall u\}$
  $(\check{\eta}, \hat{\eta}) \leftarrow (0, \check{\eta})$
  while η does not converge **do**
    $\eta \leftarrow (\check{\eta} + \hat{\eta})/2$
    Update $p_u, \forall u$ using (16)
    if $\log_2\left(1+\frac{g_{0,0}\,P_0}{\sum_{j=1}^{U} g_{0,j}\,p_j+\sigma_0^2}\right) > \frac{\tau}{1-\tau}\tilde{R}^{\mathrm{UL}}$ **then**
      $\hat{\eta} \leftarrow \eta$
    else
      $\check{\eta} \leftarrow \eta$
    end if
  end while
  $(\check{\nu}_b, \hat{\nu}_b) \leftarrow (0, \check{\nu}), \forall b$
  while $\nu_b, \forall b$ does not converge within max iteration **do**
    $\nu_b \leftarrow (\check{\nu}_b + \hat{\nu}_b)/2, \forall b$
    Update $p_u, \forall u$ using (16)
    for $b = 1, 2, \ldots, B$ **do**
      if $\sum_{u=0}^{U} \|\boldsymbol{w}_{b,u}\|^2 p_u > P^{\star}$ **then**
        $\check{\nu}_b \leftarrow \nu_b$
      else
        $\hat{\nu}_b \leftarrow \nu_b$
      end if
    end for
  end while
end while
Return: $p_u, \forall u$

$\mathcal{S} \subseteq \check{\mathcal{S}}_1$ of $\mathscr{P}_{1,\mathrm{A}}$ is reduced to $\sum_{u=0}^{U} \|\boldsymbol{w}_{b,u}\|^2 p_u \leqslant P^{\star}, \forall b$ in $\mathscr{P}_{1,\mathrm{A}}^{\mathrm{PL}}$. From the KKT conditions for the subproblem $\mathscr{P}_{1,\mathrm{A}}^{\mathrm{PL}}$, we obtain the following relation,

$$p_u = \begin{cases} \left[\frac{\eta}{t_0+\sum_{b=1}^{B}\nu_b\|\boldsymbol{w}_{b,0}\|^2\ln 2} - q_0\right]^+ & \text{if } u = 0 \\ \left[\frac{1}{t_u+\eta s_u+\sum_{b=1}^{B}\nu_b\|\boldsymbol{w}_{b,u}\|^2\ln 2} - q_u\right]^+ & \text{if } u \geqslant 1 \end{cases} \tag{16}$$

with $q_u \triangleq (\sum_{i=0,i\neq u}^{U} g_{u,i}p_i + \sigma_u^2)/g_{u,u}$, $t_u \triangleq \sum_{j=0,j\neq u}^{U} g_{j,u}\gamma_j/\rho_j$, and $s_u \triangleq g_{0,u}\gamma_0/\rho_0$, where $\rho_j = \sum_{i=0}^{U} g_{j,i}\,p_i + \sigma_j^2$ and $\gamma_j = g_{j,j}\,p_j/(\sum_{i=0,i\neq j}^{U} g_{j,i}\,p_i + \sigma_j^2)$. The function $[x]^+ \triangleq \max(x, 0)$ is used for the non-negativity of p_u.

In (16), p_u monotonically increases with η when $u = 0$ and decreases when $u \geqslant 1$ for given other variables. In other words, the log function in the rate constraint of $\mathscr{P}_{1,\mathrm{A}}$ monotonically increases with η. Hence, for given $\{\nu_b, \forall b\}$, an optimal η is found by the bisection search to satisfy the equality of the constraint. Similarly, p_u is a monotonic function of ν_b for given other variables. For each iteration, optimal $\nu_b, \forall b$ are found by the multi-dimensional bisection search to satisfy that $\sum_{u=0}^{U} \|\boldsymbol{w}_{b,u}\|^2 p_u \leqslant P^{\star}, \forall b$. The power level optimization algorithm is summarized in Algorithm 2.

V. Results

A. Simulation Setup

The random channels are realized for given positions of the nodes using the 3GPP non-terrestrial and terrestrial models in [18] and [19] as described in Sec. II-C. Specifically, the 3GPP *urban* scenario in [18] and *UMi-Street canyon* scenario in [19] are adopted at mmWave frequency with the carrier frequency of $f_{\mathrm{c}} = 30$ GHz and the bandwidth of 10 MHz. In the algorithms, we set $\check{\mu} = 10^5, \check{\eta} = 10$, and $\check{\nu} = 10$.

The GEO satellite is located at the altitude of $35,786$ km. The elevation angle between the satellite and the origin of the terrestrial network is set to be 50°. Then $d_{b,0}$ and α_b are calculated by using the relative locations of the bth gNB from the origin based on the coordinate system in [18]. The satellite is equipped with an antenna aperture of diameter 3.3 m, looking at the origin of the terrestrial network with the maximum beam gain of 58.5 dBi [2]. The antenna gain of the satellite is determined as a function of α_b. Specifically, the beam pattern model in [18, Sec. 6.4.1] is used for $G_{b,0}^{\mathrm{TX}}$ in DL and $G_{b,0}^{\mathrm{RX}}$ in UL depending on the location of the bth gNB. The transmit power of the satellite is set to be $P_0' = 50$ dBm.

In the terrestrial network, $B = 4$ gNBs are located at $(125, 125)$, $(-125, 125)$, $(-125, -125)$, and $(-125, -125)$ of the xy-plane in meter, while $U = 2$ UEs are at $(100, 30)$ and $(-40, -90)$. The heights of gNBs and UEs are 10 m and 1.5 m, respectively. The gNBs are equipped with a cylindrical array, which consists of M_{L} circular arrays each with M_{C} elements such that $M = M_{\mathrm{C}} \times M_{\mathrm{L}}$. The gNBs and UEs are assumed to have omnidirectional antenna elements. The transmit power of each UE is set to be $P_u' = 23$ dBm, $u \geqslant 1$.

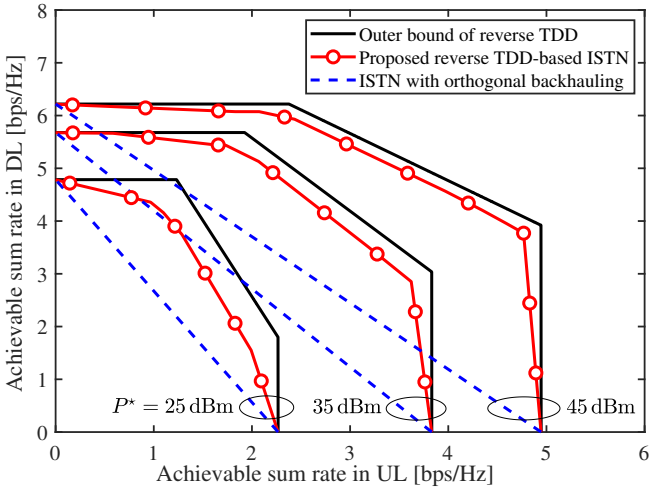

Fig. 2. UL-DL rate region for different $P^{\star}$: $M = 8 \times 2$.

B. UL-DL Rate Region of the STN with IAB

Fig. 2 presents the end-to-end UL-DL rate region obtained by varying $\zeta \in [0, 1]$. For comparison, an outer bound is presented, which assumes that the maximum transmit power $P^{\star}$ is used with optimized BF in both backhaul and access links separately with no interference between backhaul and access. Moreover, the orthogonal backhaul scheme with TDD is compared as a baseline. For this scheme, the rate region is maximized by varying the ratio between the total UL and DL periods, while optimizing time division ratios between the access UL and backhaul UL and between the access

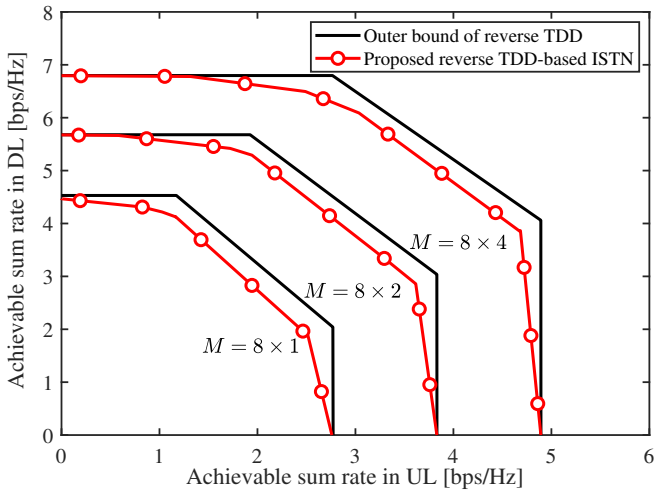

Fig. 3. UL-DL rate region for different M: $P^\star = 35\,\text{dBm}$.

DL and backhaul DL. The proposed in-band IAB system covers a significantly larger rate region than the orthogonal backhauling, while approaching to the outer bound. Note that the proposed scheme may not achieve the exact outer bound at each axis, e.g., $\zeta = 0$ and $\zeta = 1$, because of the interference from the satellite and the UEs. Fortunately, the receive BF at the gNBs mitigates those interference so that the achievable rate region is close to the outer bound. In addition, the rate region enlarges in both axes as $P^\star$ increases because a larger $P^\star$ improves both the UL and DL with adjusting τ.

Fig. 3 shows the effect of increasing M on the rate region. Since M directly affects both the receive and transmit BF gains of the gNBs at time slots 1 and 2, respectively, the rate region enlarges in both axes as M increases. Compared to the case with $P^\star = 45\,\text{dBm}$ and $M = 8 \times 2$ in Fig. 2, the case with $P^\star = 35\,\text{dBm}$ and $M = 8 \times 4$ in Fig. 3 achieves a remarkably higher rate in DL, while achieving the similar maximum UL rate. Therefore, the use of large array at the gNBs can be a power-efficient way to increase the UL-DL rate region.

VI. Conclusion

This paper introduced an in-band IAB architecture based on the reverse TDD and gNB cooperation for beyond 5G STNs. To provide high spectral efficiency, the cooperative BF and resource allocation are jointly optimized considering different rates of the backhaul and access links. Results show that the proposed in-band IAB system significantly outperforms the conventional orthogonal backhauling. In addition, the achievable UL-DL rate region approaches to that of the outer bound. The rate region can be efficiently enlarged by increasing the number of antennas at the gNBs. The trade-off between the UL and DL rates can be made by selecting appropriate weight according to data traffic demands.

Acknowledgment

The fundamental research described in this paper was supported in part by the National Research Foundation of Korea (NRF) under Grants 2021R1A6A3A14040142 and 2022R1A2C4002065, in part by the Office of Naval Research under Grant N62909-22-1-2009, and in part by the National Science Foundation under Grant CNS-2148251.

References

[1] X. Lin, S. Rommer, S. Euler, E. A. Yavuz, and R. S. Karlsson, "5G from space: An overview of 3GPP non-terrestrial networks," *IEEE Commun. Stds. Mag*, vol. 5, no. 4, pp. 147–153, Dec. 2021.

[2] 3GPP Tech. Spec. Group Radio Access Netw., "Solutions for NR to support non-terrestrial networks (NTN) (Release 16)," TR 38.821 (V16.1.0), May 2021.

[3] B. Zong, C. Fan, X. Wang, X. Duan, B. Wang, and J. Wang, "6G technologies: Key drivers, core requirements, system architectures, and enabling technologies," *IEEE Veh. Technol. Mag.*, vol. 14, no. 3, pp. 18–27, Sep. 2019.

[4] H. Saarnisaari *et al.*, "A 6G white paper on connectivity for remote areas," *arXiv preprint arXiv:2004.14699*, Apr. 2020.

[5] X. Zhu and C. Jiang, "Integrated satellite-terrestrial networks toward 6G: Architectures, applications, and challenges," *IEEE Internet of Things J.*, vol. 9, no. 1, pp. 437–461, Jan. 2022.

[6] Y. Turk and E. Zeydan, "Satellite backhauling for next generation cellular networks: Challenges and opportunities," *IEEE Commun. Mag.*, vol. 57, no. 12, pp. 52–57, Dec. 2019.

[7] 3GPP Tech. Spec. Group Radio Access Netw., "NR; Integrated access and backhaul radio transmission and reception (Release 17)," TS 38.174 (V17.1.0), Jun. 2022.

[8] G. Kwon and H. Park, "Joint user association and beamforming design for millimeter wave UDN with wireless backhaul," *IEEE J. Sel. Areas Commun.*, vol. 37, no. 12, pp. 2653–2668, Dec. 2019.

[9] B. Li, D. Zhu, and P. Liang, "Small cell in-band wireless backhaul in massive MIMO systems: A cooperation of next-generation techniques," *IEEE Trans. Wireless Commun.*, vol. 14, no. 12, pp. 7057–7069, Dec. 2015.

[10] G. Kwon and H. Park, "Beamforming design for low-power in-band wireless backhaul systems: Centralized and distributed approaches," *IEEE Trans. Veh. Technol.*, vol. 68, no. 2, pp. 1549–1563, Feb. 2019.

[11] L. You, K.-X. Li, J. Wang, X. Gao, X.-G. Xia, and B. Ottersten, "Massive MIMO transmission for LEO satellite communications," *IEEE J. Sel. Areas Commun.*, vol. 38, no. 8, pp. 1851–1865, Aug. 2020.

[12] M. A. Vazquez, L. Blanco, and A. I. Perez-Neira, "Spectrum sharing backhaul satellite-terrestrial systems via analog beamforming," *IEEE J. Sel. Topics Signal Process.*, vol. 12, no. 2, pp. 270–281, May 2018.

[13] B. Deng, C. Jiang, J. Yan, N. Ge, S. Guo, and S. Zhao, "Joint multigroup precoding and resource allocation in integrated terrestrial-satellite networks," *IEEE Trans. Veh. Technol.*, vol. 68, no. 8, pp. 8075–8090, Aug. 2019.

[14] Y. Zhang, L. Yin, C. Jiang, and Y. Qian, "Joint beamforming design and resource allocation for terrestrial-satellite cooperation system," *IEEE Trans. Commun.*, vol. 68, no. 2, pp. 778–791, Feb. 2020.

[15] Q. Wang, H. Zhang, J.-B. Wang, F. Yang, and G. Y. Li, "Joint beamforming for integrated mmwave satellite-terrestrial self-backhauled networks," *IEEE Trans. Veh. Technol.*, vol. 70, no. 9, pp. 9103–9117, Sep. 2021.

[16] L. Sanguinetti, A. L. Moustakas, and M. Debbah, "Interference management in 5G reverse TDD HetNets with wireless backhaul: A large system analysis," *IEEE J. Sel. Areas Commun.*, vol. 33, no. 6, pp. 1187–1200, Jun. 2015.

[17] A. P. Hulbert and K. D. Tomkinson, "Method of communication in a time division duplex (TDD) satellite communication system," U.S. Patent US20 070 274 249A1, 29, 2007.

[18] 3GPP Tech. Spec. Group Radio Access Netw., "Study on New Radio (NR) to support non-terrestrial networks (Release 15)," TR 38.811 (V15.4.0), Sep. 2020.

[19] ——, "Study on channel model for frequencies from 0.5 to 100 GHz (Release 16)," TR 38.901 (V16.1.0), Dec. 2019.

[20] J. Kim, H. Lee, and S. Chong, "Virtual cell beamforming in cooperative networks," *IEEE J. Sel. Areas Commun.*, vol. 32, no. 6, pp. 1126–1138, Jun. 2014.